



The Utah urban carbon dioxide (UUCON) and Uintah Basin greenhouse gas networks: Instrumentation, data and measurement uncertainty

Ryan Bares^{1,2}, Logan Mitchell¹, Ben Fasoli¹, David R. Bowling^{1,3}, Douglas Catharine¹, Maria Garcia³, Byron Eng¹, Jim Ehleringer³, John C. Lin¹

¹Department Atmospheric Sciences, University of Utah, Salt Lake City, UT, USA

²Global Change and Sustainability Center, University of Utah, Salt Lake City, UT, USA

³School of Biological Sciences, University of Utah, Salt Lake City, UT, USA

Correspondence to: Ryan Bares (ryan.bares@utah.edu)

Abstract. The Utah Urban CO₂ Network (UUCON) is a network of near-surface atmospheric carbon dioxide (CO₂) measurement sites aimed at quantifying long-term changes in urban and rural locations throughout northern Utah since 2001. We document improvements to UUCON made in 2015 that increase measurement precision, standardize sampling protocols, and expand the number of measurement locations to represent a larger region in northern Utah. In a parallel effort, near-surface CO₂ and methane (CH₄) measurement sites were assembled as part of the Uintah Basin Greenhouse Gas (GHG) network in a region of oil and natural gas extraction located in northeastern Utah. Additional efforts have resulted in automated quality control, calibration, and visualization of data through utilities hosted online (<https://air.utah.edu>). These improvements facilitate atmospheric modeling efforts and quantify atmospheric composition in urban and rural locations throughout northern Utah. Here we present an overview of the instrumentation design and methods within UUCON and the Uintah Basin GHG networks as well as describe and report measurement uncertainties using a broadly applicable and novel method. Historic and modern data described in this paper are archived with the National Oceanic and Atmospheric Administration's (NOAA) National Centers for Environmental Information (NCEI) and can be found at <https://doi.org/10.7289/V50R9MN2> and <https://doi.org/10.25921/8vaj-bk51> respectively.

1 Introduction

Increasing atmospheric carbon dioxide (CO₂) caused by anthropogenic fossil fuel combustion is the primary driver of rising global temperatures (IEA, 2015), which has led to international commitment to reduce total carbon emissions. This includes the recent Paris Climate Agreement (Rohdes, 2016) which provided a framework for countries and sub-national entities to make carbon reduction commitments. Cities are playing an increasingly prominent role in these efforts including Salt Lake City, which has committed to a 50% reduction in carbon emissions by 2030 and an 80% reduction by 2040, relative to the baseline year of 2009 (Salt Lake City Corporation, 2016). Progress on emissions reduction efforts can be evaluated with accurate greenhouse gas measurements to provide trend detection and decision support for urban stakeholders and policymakers who are assessing progress on their mitigation efforts.



Data used to study modern near-surface atmospheric CO₂ mole fraction come from a variety of sources.

35 Flask-based sampling networks such as the one led by NOAA-Earth System Research Laboratory (Tans & Conway
2005; Turnbull et al., 2012) offer long-term, globally representative records of several atmospheric tracers but can
be expensive to operate, create temporally sparse datasets, and often do not capture intra-city signals. To supplement
flask collection efforts, multiple tall tower greenhouse gas networks exist in North America (Zhao et al., 1997;
Bakwin et al., 1998; Worthy et al., 2003; Andrews et al., 2014). These networks make continuous, calibrated CO₂

40 measurements and help to fill in the temporal gaps inherent to flask-based collection. However, by design tall towers
are often located away from highly populated regions. Distance from urban emissions make tall tower measurements
an invaluable tool for regional scale analysis and background estimates, but similar to flask collection networks they
are unable to capture intra-city emissions signals.

While the majority of anthropogenic CO₂ emissions occur as a result of human activities in urban areas

45 (Hutyra, 2014; EIA, 2015), most CO₂ monitoring sites are located away from urban sources to measure well-mixed
concentrations. Thus, long-term CO₂ concentrations measured within urban areas are rare. Established in the year
2001 (Pataki et al., 2003), the Utah Urban CO₂ Network (UUCON) is the longest running multi-site urban-centric
CO₂ network in the world (Mitchell et al., 2018) (Fig. 2).

UUCON collects near-surface data used to (a) understand spatial and temporal variability of emissions

50 (Pataki 2003; Pataki et al., 2005; Mitchell et al., 2018; Bares et al., 2018), (b) evaluate the accumulation of
pollutants during complex meteorological conditions (Pataki et al., 2005; Gorski et al., 2015; Baasanborj et al.,
2017; Bares et al., 2018; Fiorella et al., 2018), (c) develop and improve atmospheric transport models (Strong et al.,
2011; Nehrkorn et al., 2013; Mallia et al., 2015), (d) validate emissions inventory estimates (McKain et al., 2012;
Bares et al., 2018), (e) investigate relationships between urban emissions and air pollution, (Baasandorj et al., 2017;

55 Mouteva et al., 2017; Bares et al., 2018), (f) and inform stakeholders and policymakers (Lin et al., 2018).

To leverage available infrastructure in urban environments and to increase the signals of intra-urban
emissions, measurement sites within UUCON are located closer to ground level (Table 1) than tall tower
measurement sites. Building-to-neighborhood-scale anthropogenic and biological fluxes contribute more strongly to
the UUCON measurements relative to remote-location flask and tall tower observations. Studies comparing tower to

60 near surface measurements in urban environments have identified an “urban canopy” effect that leads to elevated
nocturnal concentrations relative to higher above ground level (agl) measurements (Moriwaki et al., 2006). Thus, the
near-surface UUCON data are applicable to research efforts, such as near field emission studies and smaller spatial
scale analysis (~1 km² footprint, Kort et al., 2013) as well as mapping of spatial and temporal heterogeneities in
urban emissions and intra-city modeling efforts (Fasoli et al., 2018).

In recent years, cities around the world have launched efforts to establish urban near surface CO₂

65 monitoring observatories for top-down emission estimates and for modeling validation efforts similar to the
UUCON network (Mitchell et al., 2018). These cities include Los Angeles (Duren and Miller, 2012; Newman et al.,
2013; Verhulst et al., 2017), Indianapolis (Turnbull et al., 2015), Paris (Breon et al., 2015; Staufer et al., 2016),
Rome (Gratani and Varone, 2005), Davos, Switzerland (Lauvaux et al., 2013), Portland (Rice and Nostrom, 2011),

70 and Boston (Sargent et al., 2018), among others (Duren & Miller, 2012). In these studies the number of



measurement locations utilized is fewer than 5, many using a single measurement location to quantify city-wide CO₂ variability, with the notable exceptions of Indianapolis (Turnbull et al., 2015) and Los Angeles (Verhulst et al. 2017). While each of these studies employs somewhat similar measurement techniques, UUCON is unique in its length of record (Mitchell et al., 2018).

75 Starting in 2015, the University of Utah deployed a network of high frequency, high precision analyzers aimed at continuously measuring CO₂ and CH₄ from areas in eastern Utah where oil and natural gas extraction activities are prevalent (Figs. 2 and 3). These efforts were built on work previously conducted estimating fugitive CH₄ emissions (Karion et al., 2013) and the resulting local air quality problems (Edwards, 2013; Edwards et al., 2014; Koss et al., 2015). These methods have also been adopted at two UUCON sites to add CH₄ observations to the
80 urban CO₂ record.

The aim of this paper is to describe the UUCON and Uintah Basin GHG measurement procedures, site locations and data structure with sufficient detail to provide documentation for analyses using these datasets, thereby serving as an in-depth methods reference. Furthermore, we developed a novel method for exploring and quantifying the measurement uncertainty which was used to analyse the performance of the network over multiple years, to
85 provide insight into appropriate applications of the data, and to explore differences in data collection methods and instrumentation types. This unique method does not require the presence of a target tank with in the dataset, allowing for it to be broadly applicable to many trace gas and air quality datasets that are limited to calibration information alone.

2 Network Overview

90 Currently, UUCON is comprised of nine sites that are dispersed across northern Utah (Fig. 1, Table 1). Six of the sites are in the Salt Lake Valley (SLV), the most heavily populated area of Utah with over 1 million residents as of this writing and where Salt Lake City, the state capital is located. The SLV is surrounded by mountains on all sides except for the northwestern part, where it borders the Great Salt Lake (Fig. 1). Sites in the SLV span multiple characteristics and land uses including residential, mid-altitude, mixed-use industrial, and rural. Two additional sites
95 are located in the rapidly developing surrounding Heber and Cache Valleys, where the towns of Heber City and Logan are located. Both sites in the developing surrounding valleys are located in predominately residential or mixed commercial zones. In addition to the valley-based sites, a nearby high altitude CO₂ monitoring station (HDP), originally started and maintained by the National Center for Atmospheric Research as part of the Regional Atmospheric Continuous CO₂ Network in the Rocky Mountains (RACCOON; Stephens et al., 2011), has monitored
100 CO₂ levels that serve as a regional background. The HDP site transitioned into the UUCON network in Fall 2016, at which time CH₄ observations were added, and continues to be maintained by the University of Utah.

Additionally, the University of Utah maintains a network of three greenhouse gas (GHG) monitoring sites in the Uintah Basin of eastern Utah, where energy extraction is taking place, measuring both CO₂ and CH₄ (Figs. 1, 2, & 3; Table 1). The measurement techniques used in the Uintah Basin GHG network differ from UUCON in
105 several ways including the use of a different analyzer and will be discussed in detail in Sections 2.3 and 4.1. These



methods have been adapted at two sites within the UUCON network (HDP and UOU) in an effort to add more GHG measurements (CH₄) to the data record.

2.1 UUCON Instrumentation

Starting in 2001, researchers at the University of Utah deployed Li-6262 (Li-Cor inc., Lincoln, NE) infrared gas analyzers (IRGA) to measure CO₂ mole fractions in the SLV. Previous papers have described various different phases of the initial measurement sites (Pataki et al., 2003, 2005, 2006, 2007) (Fig. 2). This paper will focus on the methods and instrumentation developed in 2014 and implemented across the network by summer of 2016, as well as the methods developed for the Uintah Basin GHG network (Fig. 3). Much of the equipment and materials used during the original phase of the network informed the selection of materials for the 2015 overhaul; however, all components with the exception of the IGRA's were replaced or rebuilt completely and the methods driving these components are significantly different or improved compared to the original design. Additional components were added to increase the functionality, stability and the maintenance of measurement sites (Fig. 4).

A continuous flowing, high frequency method was developed for all locations. At each site, sample gas is continuously passed through the sample cell of a Li-6262 to measure CO₂ and H₂O mole fractions (Fig. 4, section 2.1.1). A small positive pressure is maintained throughout the analyzer and measurement system to make the identification of leaks easier and to reduce the impact on the accuracy of data in the event of a leak. Data is recorded and stored as 10-second integrations of 1-second scans.

The decision to change from the historical method, a non-continuous 5 minute collection, to the current continuous 10-second data collection was an effort to better capture higher frequency variations in observed values that could indicate near-field emissions. Additionally, high frequency data allow for easier identification of “contamination” of the measurement site from highly localized emissions (e.g., furnace, car) that can affect the signal at a site. Finally, while current atmospheric models are limited in their ability to address near field emissions effectively, advances in modeling efforts and computational resources makes this type of analysis feasible in the near future (Fasoli et al., 2018). Thus the high frequency collection of UUCON data is in anticipation of future model and analysis needs.

Multiple additional measurements are made to ensure the site's reliable performance, increase measurement accuracy, and to assist in identifying instrumentation problems when they arise (section 2.1.7). All data are downloaded and displayed in real time on a public website (<http://air.utah.edu>) to reduce the time required to identify equipment failure and to provide public outreach. Pressure and water vapor broadening corrections, as well as data calibration, are performed post data collection and will be described in depth later (section 3). Two sites in the UUCON network, UOU and HDP (Table 1), host an Ultra Portable Greenhouse Gas Analyzer (915-0011, Los Gatos Research, San Jose, CA) onsite. These sites use similar methods as those instrumented with the Li-6262 and will be discussed in-depth in section 2.2.

Lastly, the historic measurement design of UUCON included a 5-liter mixing buffer, which provided a physical mechanism for smoothing atmospheric observations and reducing instances of large deviations in



observations. After moving to a continuous flow design, the buffer has been removed to enable us to measure high frequency variations. Smoothing can still be achieved at the post-processing and data analysis stages.

2.1.1 Infrared Gas Analyzer (IRGA)

145 A Li-6262 infrared gas analyzer (IRGA) continuously measures CO₂ and H₂O mole fraction. The IRGA contains two optical measurement cells and quantifies CO₂ concentration as the difference in absorption between the two cells with a 150µm bandpass optical filter centered around 4.62µm. To achieve a concentration measurement relative to zero, a CO₂ free gas (ultra-high purity nitrogen) is flowed through the reference cell while the gas of interest is passed through the sample cell (Fig. 4).

2.1.2 Datalogger

150 A Campbell Scientific datalogger (CR1000, Campbell Scientific, Logan, UT) acts as both a measurement interface and control apparatus at each site. The datalogger records serial data streams from the gas analyzer, as well as analog voltage measurements from the gas analyzer and all additional periphery measurements. Periphery measurements include: flow rates, room temperature, sample gas pressure, sample gas temperature, and sample gas relative humidity. Several sites have additional air quality measurements that are recorded by the CR1000 (Table 1) 155 which are not discussed here. The CR1000 is also responsible for driving the calibration periphery that introduces standard gases to the IRGA every two hours (Sec. 2.1.7).

2.1.3 Pump and Sample Loop Bypass

Atmospheric sample air is pulled from the inlet to the analyzer using a 12-volt swinging piston pump (UMP850KNDC-B, KNF Neuberger Inc., Trenton, NJ) that provides a reliable flow of 3 L/min. This flow rate is 160 substantially higher than the 0.400 L/min sample flow rate selected for use at the analyzer. Thus, the pump is located upstream of the manifold where a sample loop bypass provides an alternative exit for unused sample gas. This loop is comprised of at least 9 meters of Bev-A-Line to provide sufficient resistance to the gas so when the manifold is open, gas passes through the mass flow controller and into the analyzer at the desired rate without losing all of the gas to the sample loop bypass (Fig. 4).

165 2.1.4 Relays, Manifold and Valves

Switching from sample gas to calibration gases is achieved using a six position 12-volt relay (A6REL-12, Campbell Scientific, Logan, UT), triggered by the datalogger at a known interval, connected to a six-port gas manifold (Ev/Et 6-valve, Clippard Instrument Laboratory, Inc., Cincinnati, OH) housing 12-volt Clippard relay valves (ET-2-12, Clippard Instrument Laboratory, Inc., Cincinnati, OH). Thus, when the program on the datalogger specifies, the 170 CR1000 triggers a relay closing the sample valve and introducing a gas of known CO₂ mole fraction. Since the maximum number of gases used at each sampling location is five, the unoccupied position on the relay is often used to power the atmospheric sample pump.



2.1.5 Mass Flow Controller

175 A Smart-Trek 50 mass-flow controller (Sierra Instruments, Monterey, CA) is located between the manifold and
analyzer to hold the sample flow consistent at 0.400 L/minute (Fig. 4). Flow rates are recorded by analog
measurement to the CR1000 to ensure a positive pressure remains consistent, and to help identify measurement
issues remotely.

2.1.6 Calibration Materials

180 Each site houses three whole-air, high-pressure cylinders with known CO₂ concentrations which are directly linked
to World Meteorological Organization X2007 CO₂ mole fraction scale (Zhao and Tans, 2006). Every two hours, the
three calibration tanks are introduced to the analyzer in sequence. Each transition of gas begins with a 90 second
flush period (ID -99) proceed by a 50 second measurement period, or two hours (minus calibration time) in the case
of atmospheric sampling.

185 The molar fractions of calibration gases are chosen in an effort to span expected atmospheric observations.
Values of the three reference materials are chosen to align with the 5th, 50th, and 95th percentile of the previous
year's seasonal network wide observations (Fig. 5). Utilization of previous observations as a reference allows for a
guided estimate of expected observations, thereby allowing for a minimization of interpolation without increasing
extrapolation significantly, thus limiting extrapolation bias during calibrations.

190 In addition to the standard calibration gases, a long-term target tank is introduced to the analyser every 25
hours. This tank is used to quantify performance of the site as well as determining the accuracy of post-processed
calibrated data. The interval of 25 hours was selected to ensure that the calibration occurs at a different time each
day in order to remove any consistent diel basis, and to prevent the loss of atmospheric observations at a reoccurring
time.

195 Calibration gases are produced in-house using a custom compressor design. 150-liter CGA-590 aluminum
tanks are filled with city air using a high-pressure oil free industrial compressor (SA-3 and SA-6, RIX Industries,
Benicia, CA). This system is similar to NOAA-ESRL Global Monitoring Divisions (GMD) system
(<http://www.esrl.noaa.gov/gmd/ccl/airstandard.html>). Water is removed prior to the tanks using a magnesium
perchlorate trap to guarantee a dry gas. Tanks are spiked using a ~5,000 ppm dry CO₂ tank allowing for a wide
range of targeted concentrations depending on the season and expected range of observed atmospheric observations.

200 Our facility maintains a set of nine standard tanks originally calibrated by NOAA-ESRL's GMD that range
from 328 to 800 $\mu\text{mol mol}^{-1}$ (during 2000-2004, directly linked to WMO Primary cylinders). Five of the original
laboratory primary tanks were re-measured by GMD in 2011-2012 and were found to be lower than the originally
measured CO₂ mole fraction by 0.10 to 1.52 $\mu\text{mol mol}^{-1}$.

205 Laboratory primary tanks (which span 350 – 600 $\mu\text{mol mol}^{-1}$) are propagated from the above into
“laboratory secondary” tanks using a dedicated Li-7000 (LI-COR Biosciences, Lincoln, NE), and these are used in
groups of 5 to calibrate working “tertiary” tanks used in the field. Secondary tanks are replaced as needed; since
measurements began, nine secondary tanks have been used. Secondary calibration tanks are periodically re-
measured relative to the WMO-calibrated tanks and are generally within 0.5 $\mu\text{mol mol}^{-1}$ of the original



210 measurement. To assign a known concentration number to tertiary working calibration tanks, each tank is measured
over a minimum of two days, with a minimum of three independent measurements per day. In a recent laboratory
intercomparison experiment (WMO Round Robin 6), our facilities results were within $0.1 \mu\text{mol mol}^{-1}$ of established
WMO values (https://www.esrl.noaa.gov/gmd/ccgg/wmorr/wmorr_results.php).

The same methods used for developing laboratory primary, secondary and tertiary CO_2 tanks were used for
 CH_4 calibration materials with 5 original tanks spanning from $1.489 - 9.685 \mu\text{mol mol}^{-1} \text{CH}_4$. Two of these tanks are
215 directly tied to the WMO X2004A scale (Dlugokencky et al., 2005). These tanks are propagated into laboratory
standards using a dedicated LGR-Greenhouse Gas Analyzer (Log Gatos Research, 907-0011, San Jose, CA).

A wide array of variables impact the atmospheric CO_2 mole fraction of any given urban area including
topography, fossil fuel combustion patterns, biology, and regional background conditions. Thus, intercomparison
and validation of a dataset has primarily been conducted by calibration tank round robin exercises that can tie the
220 measurements between cities to internationally accepted calibration scales and provides a high degree of confidence
in the validity of the data produced by these measurement networks.

As shown in Figures 2 & 5, winter time CO_2 concentrations in the SLV can reach over 650 ppm, with the
95th percentile over 550 ppm. As global CO_2 concentrations increase in parallel with increasing populations in the
SLV and urban areas of the Wasatch Front (Herbeke et al., 2014), the frequency and amplitude of these highly
225 elevated observations will increase. Currently the WMO X2007 CO_2 scale has a maximum mole fraction of 521.419
ppm. Thus, the current WMO scale may be inadequate for urban observations in the SLV. The urban trace gas
community should consider developing and sharing additional high-quality gas standards with mole fractions more
appropriate to urban observations.

2.1.7 Additional Measurements

230 Three additional measurement sensors were added to the downstream side of the IRGA on the sample line to
provide additional data for identifying equipment failure and to increase the accuracy of dry mole measurements. A
pressure transducer (US331-000005-015PA, Measurement Specialties Inc., Hampton, VA) is located closest to the
analyzer to represent pressures in the sample cell of the IRGA. This data stream is used for post processing pressure-
broadening and water dilution corrections. Uncertainties in the precision and long-term stability of H_2O mole
235 fraction measurements performed by the IRGA, due to a lack of frequent calibrations of water vapor, led to the
addition of a relative humidity sensor (HM1500LF, Measurement Specialties Inc., Hampton, VA) and a direct
immersion thermocouple (211M-T-U-A-2-B-1.5-N, Measurement Specialties Inc., Hampton, VA) for gas relative
humidity and temperature measurements performed immediately after the pressure transducer respectively (Fig. 4).
These measurements are utilized to calculate atmospheric H_2O ppm, which is used to calculate CO_2 dry mole and
240 correct for water vapor broadening (section 3.3).

2.1.8 Network Time Protocol

Inter-site comparison and modeling applications require a high degree of confidence in the time stamp represented
in data files. To verify the time stamps are consistent between sites and accurate, a network time check is executed



every 24 hours at 00:00 UTC. If the difference between the network clock and the clock on the datalogger is greater
245 than 1000 microseconds, the datalogger clock is reset to match the network clock. All times are recorded in UTC to
avoid potential confusion associated with daylight savings.

2.2 Uintah Basin GHG Network Instrumentation

The Uintah Basin GHG network utilizes the Los Gatos Research Ultra-Portable Greenhouse Gas Analyzer (907-
0011, Los Gatos Research Inc., San Jose, CA), hereafter referred to as “LGR” at all three sites within the network
250 (Fig. 6). The use of an “off the shelf” analyzer like the LGR compared to system like that generally employed in the
UUCON network has both advantages and disadvantages. The barrier of entry of an off the shelf unit is much lower
and does not require advanced programming abilities. However, the increase in ease of use results in a decrease in
the flexibility of operation, and in some cases the measurement precision decreases (section 4.1).

The Uintah Basin GHG network has supported several recent projects including Foster et al., 2017. In an
255 effort to minimize differences between the two instrumentation types, measurement frequency, networking, and
calibration methods and materials (sections 2.1.6) all follow the same protocols described for the UUCON network
with the notable exception of the calibration frequency, which is every three hours as opposed to every two with the
Li-6262’s.

2.2.1 LGR Calibrations

260 Calibration gases are introduced to the analyser every three hours using three whole-air, high-pressure reference gas
cylinders with known CO₂ and CH₄ concentrations that are directly linked to World Meteorological Organization
X2007 CO₂ mole fraction scale (Zhao and Tans, 2006) and the NOAA04 CH₄ mole fraction scale (Dlugokencky et
al., 2005). Calibration gases are introduced using an LGR Multiport Input Unit (MIU-9, Los Gatos Research Inc.,
San Jose, CA). H₂O mole fractions are calibrated using a Li-Cor LI- 610 dew point generator approximately every
265 three months.

2.2.2 LGR H₂O and Pressure Corrections

Corrections for pressure, water vapor dilution and spectrum broadening for CH₄ and CO₂ are made on-site by LGR’s
software and validated empirically by laboratory testing.

2.2.3 LGR Additional Considerations

270 The addition of a target tank, as described in section 2.1.6, would be greatly beneficial for analyzing the long-term
performance of each measurement site. However, the current version of the LGR proprietary software that drives the
MIU calibration unit lacks flexibility to accommodate a calibration sequence independent of a standard sequence.
Thus, the off the shelf nature makes the implementation of this somewhat more difficult.

3 Data and Post Processing



275 Raw data are pulled from each site on a 5-minute interval to the Center for Higher Performance Computing at the
University of Utah. Data are then run through an automated calibration and quality assurance program described
below and made publicly available at <https://air.utah.edu>.

3.1 Calibrations

280 Data from UUCON measurement sites with a Li-6262 on site (Table 1) are calibrated every two hours using the
three reference gases outlined in section 2.1.6, while sites with a LGR are calibrated every three hours. Since the Li-
6262's are near linear through the range of atmospheric observations and calibration gases, each standard of known
concentration is linearly interpolated between two consecutive calibration periods to represent the drift in the
measured standards over time (Fig. 7). Ordinary least squares regression is then applied to the interpolated reference
values and the linear coefficients are used to correct the observations (Fig. 7). The linear slope, intercept, and fit
285 statistics are returned for each observation for diagnostic purposes.

3.2 Pressure Corrections

Changes in ambient atmospheric pressure can impact the measurement of CO₂ mole fraction. Pressure effects can be
mathematically accounted for, or minimized or eliminated by maintaining a constant pressure in the optical cavity
during calibration and atmospheric sampling periods, as well as calibrating at a high enough frequency that
290 differences in atmospheric pressure between calibration periods is minimal. We implemented the latter of these two
strategies.

3.3 Water Vapor Calculations and Corrections

To report dry mole fractions, the presence of water vapor (H₂O) must be accounted for. The presence of water vapor
impacts measured CO₂ mole fraction through both pressure dilution and spectral band broadening. Both of these
295 effects are corrected for during the post processing of UUCON data. H₂O concentrations are calculated using the
relative humidity, pressure and temperature measurements (section 2.1.7) to first determine saturation vapor
pressure utilizing the Clausius-Clapeyron relation with Wexler's equation (Wexler, 1976) below:

$$\ln e_s = \sum_{i=0}^6 g_i T^{i-2} + g_7 \ln(T) \quad (1)$$

where e_s is the saturation vapor pressure in Pa, T is the temperature in Kelvin and coefficients $g_0 - g_7$ are as follows
300 respectively: -0.29912729×10^4 , -0.60170128×10^4 , 0.1887643854×10^2 , $-0.28354721 \times 10^{-1}$, $0.17838301 \times 10^{-4}$, $-$
 $0.84150417 \times 10^{-9}$, $0.44412543 \times 10^{-12}$, 0.2858487×10^1 .

Vapour pressure (e) is calculated using e_s from equation 1:

$$e = e_s \times \frac{RH}{100} \quad (2)$$



H₂O mixing ratio is then calculated by taking the ratio of vapor pressure (e) over total atmospheric pressure (P) and
 305 converting to parts per million (ppm).

$$H_2O = \frac{e}{P} \times 1000000 \quad (3)$$

Due to the law of partial pressures, the presence of H₂O decreases measured CO₂ mole fraction. As the amount of
 H₂O increases, the CO₂ mole fraction must decrease for atmospheric pressure to remain unchanged. Using
 calculated H₂O from equation 1, 2 and 3 we correct for the dilution effect of H₂O on the measured atmospheric CO₂
 310 using the following equation:

$$CO_{2d} = CO_{2w} \left(\frac{1}{1 - H_2O} \right) \quad (4)$$

where CO_{2w} is the “wet sample” of atmospheric CO₂ and CO_{2d} is the dry air equivalent. Given realistic atmospheric
 values for the summer in the SLV, 10,000 ppm H₂O and 400 ppm CO₂, the dilution correction described in equation
 4 will result in a positive 4.04 ppm CO₂ offset ($CO_{2d} = 404.04$ ppm).

315 The infrared absorption band utilized by the Li-6262’s deployed in the UUCON network is broadened by
 presence of H₂O resulting in a decrease in the measured CO₂ mole fraction. To correct for this effect on the
 measured CO_{2w} , described in equation 4, we calculated the CO_{2d} in equation 5:

$$Y_c(CO_{2w}) = \frac{a + b \times CO_{2w}^{1.5}}{a + CO_{2w}^{1.5}} + c \times CO_{2w}$$

$$CO_{2d} = CO_{2w}(1 + 0.5H_2O)(1 - 0.5H_2O \times Y_c(CO_{2w})) \quad (5)$$

where $a = 6606.6$, $b = 1.4306$, and $c = 2.2462 \times 10^{-4}$ and details regarding function Y_c can be found in Li-cor technical
 320 documentation (App Note #123).

Using the same values of 10,000 ppm H₂O and 400 ppm CO₂, the above equation will result in a -0.66ppm
 change. Thus the net correction for both pressure broadening (equation 4) and dilution effect (equation 5) using the
 same theoretical H₂O and CO₂ concentrations results in a 403.3 ppm CO₂ dry mole fraction.

3.4 Data Files

325 Data are stored at three different levels: raw, QA/QC, and calibrated. Data are stored in monthly files at the native
 10-second frequency for all three levels. Raw and QA/QC data files contain an identifier of which gas is currently
 being measured with atmospheric air identified as -10, flush periods as -99, and standard concentrations identified as
 their known concentration (i.e. 405.06 ppm).

330 The lowest level raw data are stored in the same format when pulled from the datalogger at the
 measurement sites. No periods of data are removed from this level and no corrections or calibrations are applied,
 thus remaining totally unaltered.

The second level of data, QAQC, remains in a similar structure as raw data with a few key exceptions.
 First, user specified bad data is removed. A text file containing the periods of “bad data” is maintained for each site,



335 which is read by automated scripts to remove selected periods. This is a fairly flexible format for removing periods
of suspect data that can be easily updated allowing for quick reprocessing of data. Second, automated quality control
scripts are run and a column of quality assurance flags are added (Table 2). Lastly, calculation of H₂O mole fraction
is performed and CO₂ dry mole fraction is calculated as described in section 3.3.

340 The third and highest level of data, calibrated data, are generated using the QAQC data files. Periods of
invalidated records that fail the automated quality control scripts are removed, and calibrations are applied to all
remaining data.

3.5 Sample Sequence

345 Since all UUCON measurement sites have only one inlet height, atmospheric sampling is continuous between
calibration periods, with no data loss associated with transition periods between sample inlets. During atmospheric
sampling, air is drawn from the inlet and passed through the analyzer continuously where it is identified (ID) as the
numerical value -10 in the raw and QA/QC data files. Every two hours, all three of the calibration materials on site
are introduced to the analyzer in sequence, with a 90 second flush period (ID = -99) to allow for equilibration and
full change-over of the sample cell, followed by 50 seconds of measurement time, resulting in a total of 140 seconds
per calibration gas. Figure 7 shows the transition from atmospheric air to a standard gas and the time required to
reach equilibration. Every 25 hours, a target tank is introduced half way through the hour (i.e., 07:30) using the same
350 sequence described above, but treated as an unknown and not utilized in the calibration routine described in section
3.1.

4 Calculating Measurement Uncertainties

A critical feature of any atmospheric measurement system is an assessment of the system's associated
measurement uncertainty. A comprehensive analysis of greenhouse gas measurement uncertainties has been
355 described for the NOAA tall tower network (Andrews et al., 2014) and for the LA Megacities project (Verhulst et
al., 2017). Here we have not estimated exhaustively every possible error source. Instead, we have focused on
creating a running uncertainty estimate through time that is similar to the approach taken in the INFLUX project
(Richardson et al., 2017) that does not include an uncertainty estimate for uncertainties from water vapor, calibration
scale reproducibility, or analyzer precision. These uncertainties are small compared to the running uncertainty
360 estimate and could be estimated in future work.

One method for estimating measurement uncertainties is to use a validation reference gas tank, or “target
tank” (U_{TGT}). The target tank is similar to the other calibration gas tanks, but it is not used to calibrate the data and is
also sampled at a lower temporal frequency (once every 25 hours; Sect. 2.1.7). An example of the target tank
measurement is shown in the right panel of Figure 7, where the target tank was measured at 07:30 UTC. The target
365 tank measurements are treated as an unknown and calibrated (section 3.1). The absolute value of the difference
between the post-calibrated and known values of the target tank is then calculated. We smoothed the absolute
difference time series by convolving it with an 11-point Gaussian window derived according to:

$$e^{-\frac{1}{2}\left(\alpha\frac{n}{(N-1)/2}\right)^2}$$



(6)

where α is 2.5, N is the number of points (11), and n is the sequence between $(N - 1)/2 \leq n \leq (N - 1)/2$. Prior studies have also used smoothed target tank values to represent measurement uncertainty through time; however, each research group has used a different method. For instance, in the NOAA tall tower network, the 1σ absolute value of the difference between the measured and known target tank mole fractions was calculated across a 3-day processing window (Andrews et al., 2014). In the LA Megacities project, the root mean square error (RMSE) across 11 target tank measurements (measured every 25 hours) was used (Verhulst et al., 2017). Finally, in the INFLUX project a running standard deviation of the absolute value of the difference between the measured and known target tank mole fractions over 30-days was used (Richardson et al., 2017). While these approaches differ in their details, each represents an assessment of U_{TGT} through time. Future work could examine how the different target tank-based uncertainty estimates compare to each other and how they affect atmospheric inversion estimates.

Within the UUCON network, target tanks were incorporated into the experimental design in July 2017 at all of the sites with a Li-6262 analyzer, while sites equipped with a LGR analyzer did not host a target tank, as of this writing. Thus, to estimate the measurement uncertainty at the LGR sites as well as at Li-6262 sites prior to the deployment of the target tanks, an alternative measurement uncertainty method was needed. We produced a method that takes the calibration gas measurements at time t , treats them as pseudo target tanks, and interpolates the calibration gas measurements between the prior ($t-1$) and next ($t+1$) calibration periods to derive a slope and intercept at time t that is then used to calculate the calibrated mole fraction mixing ratios of the pseudo target tanks and derive an uncertainty estimate. An example of this process is shown in Figure 8 for the calibration on Nov 27, 2017 at 18:00 UTC at the IMC site. The calibration gas measurements were interpolated between 16:00 ($t-1$) and 20:00 ($t+1$) and used to obtain an interpolated slope and intercept at 18:00 (t) (blue dashed line and triangles in Fig. 8a). The interpolated slope and intercept can be compared to the actual values obtained from the usual calibration procedure (orange circles). The blue dashed line illustrating the interpolation procedure is only shown between 16:00 and 20:00 for clarity, but this process was repeated for each calibration time period. The interpolated slope and intercept were then used to calibrate the pseudo target tank measurements at t (blue triangles in Fig. 8b). The RMSE between the calibrated and known values of the three pseudo target tanks was then calculated (grey circles in Fig. 8d). Since the RMSE can vary substantially between calibration points, we smoothed it by convolving it with an 11-point Gaussian window to yield the pseudo target tank uncertainty, or U_{pTGT} (blue circles in Fig. 8d). For this example at 18:00, the interpolated calibration intercept resulted in a relatively large deviation of the calibrated pseudo target tank mole fractions from their known values that then resulted in an elevated RMSE. The elevated RMSE from this calibration point then persists for several calibration periods (hours) in the smoothed U_{pTGT} .

Once U_{pTGT} was calculated, we compared it to the traditional U_{TGT} over time at the IMC site (Fig. 9). For reference, the yellow shaded region in Figure 9 is the time period shown in Figure 8. In July-August 2017 at IMC there was a bias in the calibrated target tank mole fractions that similarly affected the pseudo target tank RMSE values (Fig. 8d). In September 2017 the third calibration tank was removed from the site for a month and the RMSE values of both metrics improved. Finally, in October 2017 a third calibration tank was re-installed and there was again a bias in the target tank and pseudo target tanks. The close fidelity through time between the U_{pTGT} and U_{TGT}



405 metrics provides confidence that U_{pTGT} serves as a robust estimate of measurement uncertainty that is similar to what
can be obtained with a traditional target tank. Finally, Figure 10 shows the entire CO_2 U_{pTGT} and U_{TGT} record at all
of the sites, while Figure 11 shows the entire CH_4 U_{pTGT} record. The U_{pTGT} is reported in the hourly averaged data
files as our estimate of measurement uncertainty.

The average absolute difference between U_{pTGT} and U_{TGT} at all sites in the UUCON network was 0.18 ppm
410 CO_2 , suggesting this metric is representative of a more directly measured uncertainty metric like U_{TGT} .

4.1 Instrument Differences and Uncertainties

A unique aspect of the UUCON and Uintah Basin networks is the use of two different instruments to
measure CO_2 . This allows the ability to directly compare instrument performance during extended field operations.
Table 3 shows the uncertainty metrics described in section 4 and in Figures 8, 9, 10 and 11. Additionally, the
415 precision of the instruments (U_p) at each site is reported as an average value of the standard deviation (1σ) of the
post calibrated values for each individual calibration gas introduced to the analyzer since the overhaul of the site, as
well as the data recovery rates for each site. Site to site variability in U_{pTGT} ranges from 0.17 to 0.70 ppm CO_2 within
the UUCON network, with the highest observed uncertainty at sites with more limited environmental controls. Sites
equipped with a LGR ranged from 0.17 to 0.32 CO_2 ppm (1.8 to 3.3 ppb CH_4), with a mean across all sites of 0.27
420 ppm CO_2 (2.8 ppb CH_4).

Our reported average CH_4 U_{pTGT} uncertainty value of 2.8 ppb is notably higher than those reported by other
groups quantifying measurement uncertainty, including Verhulst et al., 2017 which reported a value of 0.2126 ppb
uncertainty as estimated using the post-calibrated target tank residuals integrated over 10 days of observations, and a
total CH_4 uncertainty (U_{air}) of 0.7224 ppm from measurements using a Picarro G2301 (Picarro Inc., Santa Clara,
425 CA). Our higher reported values are likely the result of both the use of a different analyzer than a Picarro, as well as
the fact that our uncertainty estimates are based on an interpolation between non-sequential calibration periods and
not a directly measured target tank.

It is notable that in all but one instance that the precision (U_p) of the Li-6262s CO_2 is twice as precise than
the LGRs (Table 3), and the one instance is at DBK which experiences larger temperature ranges, despite the Li-
430 6262s being ~20 years older than the LGRs. Additionally, the uncertainty and data recovery rates between the two
instrument types are highly comparable.

The highly similar CO_2 metrics observed between the two instrumentation types suggests that the most
significant advantage of the more modern direct absorption LGR's is the addition of a second gas species measured,
methane (CH_4) in this instance, especially at sites with well-regulated climate controls.

435 5 Data Availability

All data described in this paper are archived with the National Oceanic and Atmospheric Administration's
(NOAA) National Centers for Environmental Information (NCEI) and can be found at <https://doi.org/10.7289/V50R9MN2> and <https://doi.org/10.25921/8vaj-bk51>.



6 Conclusions

440 As the global effort to reduce greenhouse gas emissions transitions from commitment to policy measures, greenhouse gas measurement networks provide a means for evaluating progress. The UUCON network is an example of an urban CO₂ network well suited for this application due to its long-term duration, precision, and spatial distribution (Mitchell et al., 2018). With high data recovery rates and low average measurement uncertainty (U_{pTGT}) of 0.37 ppm CO₂, the network produces data suitable for a range of scientific and, potentially, policy applications.

445 Additionally, there is increasing interest in performing cross-urban comparisons between different urban environments. Given the reported measurement uncertainties, the frequency of calibrations and the tractability to international working scales, these data are well situated for this application.

The overhaul of instrumentation and design documented in this paper has resulted in a robust network of reliable data, with additional measurements to remotely identify when problems arise as well as increase the
450 precision of the data. The standardization of materials and measurement protocols at all locations has significantly lowered the barrier of entry for maintenance of the sites.

The addition of target tanks at multiple sites in 2017 allows for the calculation of continuous uncertainty metrics. From those metrics, an interpolation method was developed allowing for uncertainty estimates of sites and networks where a target tank is not available. While this method likely results in overestimation in the uncertainty,
455 this novel method for estimating uncertainty nonetheless provides useful insight into the quality of data produced at individual sites and is broadly applicable to any atmospheric trace gas or air quality dataset that contains calibration information.

The use of the interpolated uncertainty metric, as well as the calculation of the standard deviation of calibration measurements in the field, identified limited differences between the two measurement techniques used
460 in the UUCON and Uintah Basin GHG networks.

Targeted reductions in the emissions of other greenhouse gases, primarily CH₄, will require similarly distributed measurement networks for validating reduction progress and tracking emissions, both in urban areas and regions of oil and natural gas extraction. With three years of continuous operation to date, and relatively low measurement uncertainty (2.8 ppb CH₄) the Uintah Basin GHG network serves as a good example of a greenhouse
465 gas network with simultaneous measurements of CH₄ and CO₂. With comparable precision and reliability as those reported in UUCON, but with the added benefit of two measurement species, the measurement techniques deployed in the Uintah Basin GHG network have been expanded into a few urban locations within the UUCON network.

Acknowledgements

470 This research was supported by the National Oceanic and Atmospheric Administration (NOAA) grant NA140AR4310178 and NA140AR4310138. The authors would like to thank Dr. Britton Stephens and the National Center for Atmospheric Research for establishing the HDP site, Dr. Seth Lyman and Utah State University-Vernal for their continued support of the Uintah Basin GHG network, and The Stable Isotope Ratio Facility for Environmental Research (SIRFER) at the University of Utah for their commitment to UUCON. We would also like
475 to thank the following hosting institutions: Draper City and the Salt Lake County Unified Fire Authority, Rio Tinto



Kennecott, Snowbird Ski Resort, The Salt Lake Center of Science Education, Intermountain Health Center, Utah State University Logan, Utah State University Vernal, Wasatch County Health Department, and the Utah Division of Air Quality. All data used in this analysis are available upon request from the corresponding author or can be downloaded at the U-ATAQ's data repository at <https://air.utah.edu/data/>.

480 **References**

- Ahmadov, R., McKeen, S., Trainer, M., Banta, R., Brewer, A., Brown, S., Edwards, P. M., De Gouw, J. A., Frost, G. J., Gilman, J., Helmig, D., Johnson, B., Karion, A., Koss, A., Langford, A., Lerner, B., Olson, J., Oltmans, S., Peischl, J., Pétron, G., Pichugina, Y., Roberts, J. M., Ryerson, T., Schnell, R., Senff, C., Sweeney, C., Thompson, C., Veres, P. R., Warneke, C., Wild, R., Williams, E. J., Yuan, B. and Zamora, R.: Understanding high wintertime ozone pollution events in an oil- and natural gas-producing region of the western US, *Atmospheric Chemistry and Physics*, 15(1), 411–429, doi:10.5194/acp-15-411-2015, 2015.
- 485 Andrews, A. E., Kofler, J. D., Trudeau, M. E., Williams, J. C., Neff, D. H., Masarie, K. A., Chao, D. Y., Kitzis, D. R., Novelli, P. C., Zhao, C. L., Dlugokencky, E. J., Lang, P. M., Crotwell, M. J., Fischer, M. L., Parker, M. J., Lee, J. T., Baumann, D. D., Desai, A. R., Stanier, C. O., De Wekker, S. F. J., Wolfe, D. E., Munger, J. W. and Tans, P. P.: CO₂, CO, and CH₄ measurements from tall towers in the NOAA earth system research laboratory's global greenhouse gas reference network: Instrumentation, uncertainty analysis, and recommendations for future high-accuracy greenhouse gas monitoring efforts, *Atmospheric Measurement Techniques*, 7(2), 647–687, doi:10.5194/amt-7-647-2014, 2014.
- 490 App Note #123. Implementing Zero and Span Adjustments, and the Band Broadening Correction On Measured Data, 3576(1), 1–6. <https://www.licor.com/documents/6yqgna9zt7y6avvg2azs>
- 495 Baasandorj, M., Hoch, S. W., Bares, R., Lin, J. C., Brown, S. S., Millet, D. B., Martin, R., Kelly, K., Zarzana, K. J., Whiteman, C. D., Dube, W. P., Tonnesen, G., Jaramillo, I. C. and Sohl, J.: Coupling between Chemical and Meteorological Processes under Persistent Cold-Air Pool Conditions: Evolution of Wintertime PM_{2.5} Pollution Events and N₂O₅ Observations in Utah's Salt Lake Valley, *Environmental Science and Technology*, 51(11), 5941–5950, doi:10.1021/acs.est.6b06603, 2017.
- 500 Bakwin, P. S., Tans, P. P., Hurst, D. F. and Zhao, C.: Measurements of carbon dioxide on very tall towers : results of the NOAA / CMDL program, *Tellus*, 50(December), 401–415, doi:10.1034/j.1600-0889.1998.t01-4-00001.x, 1998.
- Bares, Ryan; Lin, John C.; Fasoli, Ben; Mitchell, Logan E.; Bowling, David R.; Garcia, Maria; Catharine, Douglas; Ehleringer, James R. (2018). Atmospheric measurements of carbon dioxide (CO₂) and methane (CH₄) from the state of Utah from 2014-09-10 to 2018-04-01 (NCEI Accession 0183632). Version 1.1. NOAA National Centers for Environmental Information. Dataset. doi:10.25921/8vaj-bk51
- 505 Bares, R., Lin, J. C., Hoch, S. W., Baasandorj, M., Mendoza, D. L., Fasoli, B., Mitchell, L., Catharine, D. and Stephens, B. B.: The Wintertime Covariation of CO₂ and Criteria Pollutants in an Urban Valley of the Western United States, *Journal of Geophysical Research: Atmospheres*, (2), 1–20, doi:10.1002/2017JD027917, 2018.
- 510 Bowling, D. R., Burns, S. P., Conway, T. J., Monson, R. K. and White, J. W. C.: Extensive observations of CO₂ carbon isotope content in and above a high-elevation subalpine forest, *Global Biogeochemical Cycles*, 19(3), 1–15, doi:10.1029/2004GB002394, 2005.
- Breón, F. M., Broquet, G., Puygrenier, V., Chevallier, F., Xueref-Remy, I., Ramonet, M., Dieudonné, E., Lopez, M., Schmidt, M., Perrussel, O. and Ciais, P.: An attempt at estimating Paris area CO₂ emissions from atmospheric concentration measurements, *Atmospheric Chemistry and Physics*, 15(4), 1707–1724, doi:10.5194/acp-15-1707-2015, 2015.
- 515 Briber, B., Hutyra, L., Dunn, A., Raciti, S. and Munger, J.: Variations in Atmospheric CO₂ Mixing Ratios across a Boston, MA Urban to Rural Gradient, *Land*, 2(3), 304–327, doi:10.3390/land2030304, 2013. D. V. Mallia, J. C. Lin, S. Urbanski, J. Ehleringer, and T. N.: Impacts of upwind wildfire emissions on CO, CO₂, and PM_{2.5} concentrations in Salt Lake City, Utah, *Journal of Geophysical Research : Atmospheres*, 147–166, doi:10.1002/2017JC013052, 2015.
- 520 Deadline 2020 - how cities will get the job done. [online] Available from: http://c40-production-images.s3.amazonaws.com/researches/images/59_C40_Deadline_2020_Report.original.pdf?1480609788, 2018.



- 525 Dlugokencky, E. J., Myers, R. C., Lang, P. M., Masarie, K. A., Crotwell, A. M., Thoning, K. W., Hall, B. D., Elkins, J. W. and Steele, L. P.: Conversion of NOAA atmospheric dry air CH₄ mole fractions to a gravimetrically prepared standard scale, *Journal of Geophysical Research D: Atmospheres*, 110(18), 1–8, doi:10.1029/2005JD006035, 2005.
- Duren, R. M. and Miller, C. E.: Measuring the carbon emissions of megacities, *Nature Climate Change*, 2, 560 [online] Available from: <http://dx.doi.org/10.1038/nclimate1629>, 2012. Duren, R. M., & Miller, C. E.: Measuring the carbon emissions of megacities. *Nature Climate Change*, 2, 560. Retrieved from <http://dx.doi.org/10.1038/nclimate1629>, 2012.
- 530 Edwards, P. M., Young, C. J., Aikin, K., DeGouw, J., Dubé, W. P., Geiger, F., Gilman, J., Helmig, D., Holloway, J. S., Kercher, J., Lerner, B., Martin, R., McLaren, R., Parrish, D. D., Peischl, J., Roberts, J. M., Ryerson, T. B., Thornton, J., Warneke, C., Williams, E. J. and Brown, S. S.: Ozone photochemistry in an oil and natural gas extraction region during winter: Simulations of a snow-free season in the Uintah Basin, Utah, *Atmospheric Chemistry and Physics*, 13(17), 8955–8971, doi:10.5194/acp-13-8955-2013, 2013.
- 535 Edwards, P. M., Brown, S. S., Roberts, J. M., Ahmadov, R., Banta, R. M., DeGouw, J. A., Dubé, W. P., Field, R. A., Flynn, J. H., Gilman, J. B., Graus, M., Helmig, D., Koss, A., Langford, A. O., Lefer, B. L., Lerner, B. M., Li, R., Li, S. M., McKeen, S. A., Murphy, S. M., Parrish, D. D., Senff, C. J., Soltis, J., Stutz, J., Sweeney, C., Thompson, C. R., Trainer, M. K., Tsai, C., Veres, P. R., Washenfelder, R. A., Warneke, C., Wild, R. J., Young, C. J., Yuan, B. and Zamora, R.: High winter ozone pollution from carbonyl photolysis in an oil and gas basin, *Nature*, 514(7522), 351–354, doi:10.1038/nature13767, 2014.
- Fasoli, B., Lin, J. C., Bowling, D. R., Mitchell, L. and Mendoza, D.: Simulating atmospheric tracer concentrations for spatially distributed receptors: Updates to the Stochastic Time-Inverted Lagrangian Transport model's R interface (STILT-R version 2), *Geoscientific Model Development*, 11(7), 2813–2824, doi:10.5194/gmd-11-2813-2018, 2018.
- 545 Foster, C. S., Crosman, E. T., Holland, L., Mallia, D. V., Fasoli, B., Bares, R., Horel, J. and Lin, J. C.: Confirmation of elevated methane emissions in Utah's Uintah Basin with ground-based observations and a high-resolution transport model, *Journal of Geophysical Research: Atmospheres*, 1–19, doi:10.1002/2017JD027480, 2017.
- 550 Fiorella, R. P., Bares, R., Lin, J. C., Ehleringer, J. R., & Bowen, G. J.: Detection and variability of combustion-derived vapor in an urban basin. *Atmospheric Chemistry and Physics Discussions*, 1–26. <http://doi.org/10.5194/acp-2017-1106>, 2018
- Foster, C. S., Crosman, E. T., Holland, L., Mallia, D. V., Fasoli, B., Bares, R., Horel, J. and Lin, J. C.: Confirmation of elevated methane emissions in Utah's Uintah Basin with ground-based observations and a high-resolution transport model, *Journal of Geophysical Research: Atmospheres*, 1–19, doi:10.1002/2017JD027480, 2017.
- 555 Gorski, G., Strong, C., Good, S. P., Bares, R., Ehleringer, J. R. and Bowen, G. J.: Vapor hydrogen and oxygen isotopes reflect water of combustion in the urban atmosphere, *Proceedings of the National Academy of Sciences*, 112(11), 3247–3252, doi:10.1073/pnas.1424728112, 2015.
- Gratani, L. and Varone, L.: Daily and seasonal variation of CO in the city of Rome in relationship with the traffic volume, *Atmospheric Environment*, 39(14), 2619–2624, doi:10.1016/j.atmosenv.2005.01.013, 2005.
- 560 Hutyra, L. R., Duren, R., Gurney, K. R., Grimm, N., Kort, E. A., Larson, E. and Shrestha, G.: Urbanization and the carbon cycle: Current capabilities and research outlook from the natural sciences perspective, *Earth's Future*, 2(10), 473–495, doi:10.1002/2014EF000255, 2014.
- IEA: Energy and Climate Change, *World Energy Outlook Special Report*, 1–200, doi:10.1038/479267b, 2015.
- 565 Karion, A., Sweeney, C., Pétron, G., Frost, G., Michael Hardesty, R., Kofler, J., Miller, B. R., Newberger, T., Wolter, S., Banta, R., Brewer, A., Dlugokencky, E., Lang, P., Montzka, S. A., Schnell, R., Tans, P., Trainer, M., Zamora, R. and Conley, S.: Methane emissions estimate from airborne measurements over a western United States



- natural gas field, *Geophysical Research Letters*, 40(16), 4393–4397, doi:10.1002/grl.50811, 2013.
- 570 Kort, E. A., Angevine, W. M., Duren, R. and Miller, C. E.: Surface observations for monitoring urban fossil fuel CO₂ emissions: Minimum site location requirements for the Los Angeles megacity, *Journal of Geophysical Research Atmospheres*, 118(3), 1–8, doi:10.1002/jgrd.50135, 2013.
- Koss, A. R., De Gouw, J., Warneke, C., Gilman, J. B., Lerner, B. M., Graus, M., Yuan, B., Edwards, P., Brown, S. S., Wild, R., Roberts, J. M., Bates, T. S. and Quinn, P. K.: Photochemical aging of volatile organic compounds associated with oil and natural gas extraction in the Uintah Basin, UT, during a wintertime ozone formation event, *Atmospheric Chemistry and Physics*, 15(10), 5727–5741, doi:10.5194/acp-15-5727-2015, 2015.
- 575 Lauvaux, T., Miles, N. L., Richardson, S. J., Deng, A., Stauffer, D. R., Davis, K. J., Jacobson, G., Rella, C., Calonder, G. P. and Decola, P. L.: Urban emissions of CO₂ from Davos, Switzerland: The first real-time monitoring system using an atmospheric inversion technique, *Journal of Applied Meteorology and Climatology*, 52(12), 2654–2668, doi:10.1175/JAMC-D-13-038.1, 2013.
- 580 Lin, J.C., L. Mitchell, E. Crosman, D. Mendoza, M. Buchert, R. Bares, B. Fasoli, D.R. Bowling, D. Pataki, D. Catharine, C. Strong, K. Gurney, R. Patarasuk, M. Baasandorj, A. Jacques, S. Hoch, J. Horel, and J. Ehleringer.: [CO₂ and carbon emissions from cities: linkages to air quality, socioeconomic activity and stakeholders in the Salt Lake City urban area](https://doi.org/10.1175/BAMS-D-17-0037.1). *Bull. Amer. Meteor. Soc.*, 0, <https://doi.org/10.1175/BAMS-D-17-0037.1>, 2018.
- 585 Mallia, D.V, Lin, J. C., Urbanski, S., Ehleringer, J., T. N. : Impacts of upwind wildfire emissions on CO, CO₂, and PM_{2.5} concentrations in Salt Lake City, Utah. *Journal of Geophysical Research : Atmospheres*, 147–166. <http://doi.org/10.1002/2017JCO13052>, 2015.
- McKain, K., Wofsy, S. C., Nehrkorn, T., Eluszkiewicz, J., Ehleringer, J. R. and Stephens, B. B.: Assessment of ground-based atmospheric observations for verification of greenhouse gas emissions from an urban region., *Proceedings of the National Academy of Sciences of the United States of America*, 109(22), 8423–8, doi:10.1073/pnas.1116645109, 2012.
- 590 Mitchell, L. E., Lin, J. C., Bowling, D. R., Pataki, D. E., Strong, C., Schauer, A. J., Bares, R., Bush, S. E., Stephens, B. B., Mendoza, D., Mallia, D., Holland, L., Gurney, K. R. and Ehleringer, J. R.: Long-term urban carbon dioxide observations reveal spatial and temporal dynamics related to urban characteristics and growth, *Proceedings of the National Academy of Sciences of the United States of America*, 115(12), doi:10.1073/pnas.1702393115, 2018.
- 595 Mitchell, Logan E.; Lin, John C.; Bowling, David R.; Pataki, Diane E.; Strong, Courtenay; Schauer, Andrew J.; Bares, Ryan; Bush, Susan E.; Stephens, Britton B.; Mendoza, Daniel; Mallia, Derek; Holland, Lacey; Gurney, Kevin R.; Ehleringer, James R.: Carbon Dioxide (CO₂) mole fraction, CO₂ flux, and others collected from Salt Lake City CO₂ measurement network in Western U.S. from 2001-02-07 to 2015-10-23 (NCEI Accession 0170450). Version 1.1. NOAA National Centers for Environmental Information. Dataset. doi:10.7289/V50R9MN2, 2018.
- 600 Mitchell, L. E., Crosman, E. T., Jacques, A. A., Fasoli, B., Leclair-Marzolf, L., Horel, J., Bowling, D. R., Ehleringer, J. R. and Lin, J. C.: Monitoring of greenhouse gases and pollutants across an urban area using a light-rail public transit platform, *Atmospheric Environment*, 187(May), 9–23, doi:10.1016/j.atmosenv.2018.05.044, 2018.
- Moriwaki, R., Kanda, M. and Nitta, H.: Carbon dioxide build-up within a suburban canopy layer in winter night, *Atmospheric Environment*, 40(8), 1394–1407, doi:10.1016/j.atmosenv.2005.10.059, 2006.
- 605 Mouteva, G. O., Randerson, J. T., Fahrni, S. M., Bush, S. E., Ehleringer, J. R., Xu, X., Santos, G. M., Kuprov, R., Schichtel, B. A. and Czimeczik, C. I.: Using radiocarbon to constrain black and organic carbon aerosol sources in Salt Lake City, *Journal of Geophysical Research: Atmospheres*, 122(18), 9843–9857, doi:10.1002/2017JD026519, 2017.
- Nehrkorn, T., Henderson, J., Leidner, M., Mountain, M., Eluszkiewicz, J., McKain, K. and Wofsy, S.: WRF simulations of the urban circulation in the salt lake city area for CO₂ modeling, *Journal of Applied Meteorology and*



- 610 *Climatology*, 52(2), 323–340, doi:10.1175/JAMC-D-12-061.1, 2013.
- Nehrkorn, T., Henderson, J., Leidner, M., Mountain, M., Eluszkiewicz, J., McKain, K. and Wofsy, S.: WRF simulations of the urban circulation in the salt lake city area for CO₂ modeling, *Journal of Applied Meteorology and Climatology*, 52(2), 323–340, doi:10.1175/JAMC-D-12-061.1, 2013.
- 615 Newman, S., Jeong, S., Fischer, M. L., Xu, X., Haman, C. L., Lefer, B., Alvarez, S., Rappenglueck, B., Kort, E. A., Andrews, A. E., Peischl, J., Gurney, K. R., Miller, C. E. and Yung, Y. L.: Diurnal tracking of anthropogenic CO₂ emissions in the Los Angeles basin megacity during spring 2010, *Atmospheric Chemistry and Physics*, 13(8), 4359–4372, doi:10.5194/acp-13-4359-2013, 2013.
- Pataki, D. E., Bowling, D. R., Ehleringer, J. R.: Seasonal cycle of carbon dioxide and its isotopic composition in an urban atmosphere: Anthropogenic and biogenic effects, *Journal of Geophysical Research*, 108(D23), 4735, doi:10.1029/2003JD003865, 2003.
- 620 Pataki, D. E., Bowling, D. R., Ehleringer, J. R. and Zobitz, J. M.: High resolution atmospheric monitoring of urban carbon dioxide sources, *Geophysical Research Letters*, 33(3), 1–5, doi:10.1029/2005GL024822, 2006.
- Pataki, D. E., Tyler, B. J., Peterson, R. E., Nair, A. P., Steenburgh, W. J. and Pardyjak, E. R.: Can carbon dioxide be used as a tracer of urban atmospheric transport?, *Journal of Geophysical Research D: Atmospheres*, 110(15), 1–8, doi:10.1029/2004JD005723, 2005.
- 625 Pataki, D. E., Xu, T., Luo, Y. Q. and Ehleringer, J. R.: Inferring biogenic and anthropogenic carbon dioxide sources across an urban to rural gradient, *Oecologia*, 152(2), 307–322, doi:10.1007/s00442-006-0656-0, 2007.
- Rhodes, C. J.: The 2015 Paris climate change conference: COP21, *Science Progress*, 99(1), 97–104, doi:10.3184/003685016X14528569315192, 2016.
- 630 Rice, A. and Bostrom, G.: Measurements of carbon dioxide in an Oregon metropolitan region, *Atmospheric Environment*, 45(5), 1138–1144, doi:10.1016/j.atmosenv.2010.11.026, 2011.
- Salt Lake City Corporation. A joint resolution of the Salt Lake City Council and Mayor Establishing Renewable Energy and Carbon Emissions Reduction Goals for Salt Lake City. 206
- 635 Sargent, M., Barrera, Y., Nehrkorn, T., Hutyla, L. R., Gately, C. K., Jones, T., McKain, K., Sweeney, C., Hegarty, J., Hardiman, B. and Wofsy, S. C.: Anthropogenic and biogenic CO₂ fluxes in the Boston urban region, *Proceedings of the National Academy of Sciences*, 115(29), 7491–7496, doi:10.1073/pnas.1803715115, 2018.
- Staufner, J., Broquet, G., Bréon, F.-M., Puygrenier, V., Chevallier, F., Xueref-Rémy, I., Dieudonné, E., Lopez, M., Schmidt, M., Ramonet, M., Perrussel, O., Lac, C., Wu, L. and Ciais, P.: A first year-long estimate of the Paris region fossil fuel CO₂ emissions based on atmospheric inversion, *Atmospheric Chemistry and Physics Discussions*, (April), 1–34, doi:10.5194/acp-2016-191, 2016.
- 640 Stephens, B. B., Miles, N. L., Richardson, S. J., Watt, A. S. and Davis, K. J.: Atmospheric CO₂ monitoring with single-cell NDIR-based analyzers, *Atmospheric Measurement Techniques*, 4(12), 2737–2748, doi:10.5194/amt-4-2737-2011, 2011.
- 645 Strong, C., Stwertka, C., Bowling, D. R., Stephens, B. B. and Ehleringer, J. R.: Urban carbon dioxide cycles within the Salt Lake Valley: A multiple-box model validated by observations, *Journal of Geophysical Research Atmospheres*, 116(15), 1–12, doi:10.1029/2011JD015693, 2011.
- Tabuchi H, Fountain H.: Bucking Trump, these cities, states and companies commit to Paris accord. *NY Times*, Section A, p 12., 2017



- 650 Tans, Pieter P. and T.J. Conway,: Monthly Atmospheric CO₂ Mixing Ratios from the NOAA CMDL Carbon Cycle Cooperative Global Air Sampling Network, 1968-2002. In Trends: A Compendium of Data on Global Change. Carbon Dioxide Information Analysis Center, Oak Ridge National Laboratory, U.S. Department of Energy, Oak Ridge, Tenn., U.S.A., 2005.
- 655 Turnbull, J., Guenther, D., Karion, A., Sweeney, C., Anderson, E., Andrews, A., Kofler, J., Miles, N., Newberger, T., Richardson, S. and Tans, P.: An integrated flask sample collection system for greenhouse gas measurements, *Atmospheric Measurement Techniques*, 5(9), 2321–2327, doi:10.5194/amt-5-2321-2012, 2012.
- Turnbull, J. C., Sweeney, C., Karion, A., Newberger, T., Lehman, S. J., Cambaliza, M. O., Shepson, P. B., Gurney, K., Patarasuk, R. and Razlivanov, I.: Toward quantification and source sector identification of fossil fuel CO₂ emissions from an urban area: Results from the INFLUX experiment, *Journal of Geophysical Research : Atmospheres*, (120), 292–312, doi:10.1002/2014JD022555. Received, 2015.
- 660 Turner, A. J., Shusterman, A. A., McDonald, B. C., Teige, V., Harley, R. A. and Cohen, R. C.: Network design for quantifying urban CO₂ emissions: Assessing trade-offs between precision and network density, *Atmospheric Chemistry and Physics*, 16(21), 13465–13475, doi:10.5194/acp-16-13465-2016, 2016.
- 665 Verhulst, K. R., Karion, A., Kim, J., Salameh, P. K., Keeling, R. F., Newman, S., Miller, J., Sloop, C., Pongetti, T., Rao, P., Wong, C., Hopkins, F. M., Yadav, V., Weiss, R. F., Duren, R. M. and Miller, C. E.: Carbon dioxide and methane measurements from the Los Angeles Megacity Carbon Project - Part I: Calibration, urban enhancements, and uncertainty estimates, *Atmospheric Chemistry and Physics*, 17(13), 8313–8341, doi:10.5194/acp-17-8313-2017, 2017.
- Wexler, A.: Vapor Pressure Equation for Water in Range 3 To 100 Degrees C. *Journal of Research of the National Bureau of Standards - A. Physics and Chemistry*, 80A(3), 775–785. <http://doi.org/10.6028/jres.075A.022>, 1976.
- 670 Worthy, D. E. J., Platt, A., Kessler, R., Ernst, M., Braga, R., and Racki, S.: The Canadian atmospheric carbon dioxide measurement program: Measurement procedures, data quality and accuracy, In: Report of the 11th WMO/IAEA Meeting of Experts on Carbon Dioxide Concentration and Related Tracer Measurement Techniques, Tokyo, Japan, September 2001, edited by: Toru, S. and Kazuto, S., World Meteorological Organization Global Atmosphere Watch, 112–128, 2003
- 675 Zhao, C. L., Bakwin, P. S. and Tans, P. P.: A design for unattended monitoring of carbon dioxide on a very tall tower, *Journal of Atmospheric and Oceanic Technology*, 14(5), 1139–1145, doi:10.1175/1520-0426(1997)014<1139:ADFUMO>2.0.CO;2, 1997.
- Zhao, C. L. and Tans, P. P.: Estimating uncertainty of the WMO mole fraction scale for carbon dioxide in air, *Journal of Geophysical Research Atmospheres*, 111(8), 1–10, doi:10.1029/2005JD006003, 2006.



680

Table 1: Site Characteristics of the UUCON (top) and Uintah Basin GHG network (bottom). Historic sites that have been relocated are not listed. Details regarding instrument types and measurement details for species other than CO₂ and CH₄ are not covered in this paper but currently measured at a subset of sites include Carbon Monoxide (CO), Ozone (O₃), Fine particulate Matter (PM_{2.5}) and Nitrogen Oxides (NO_x).

Site Code	Site Name	Latitude	Longitude	Elevation (m)	Inlet Height (m agl)	Species	Start Year	Overhaul Year	Instrument	Land-Use
UOU	University of Utah	40.7663	111.8478	1,436	36.2	CO ₂ , CH ₄ , CO, O ₃ , PM _{2.5} , NO _x	2001	2014	LGR UP-GGA	Mixed residential commercial
SUG	Sugarhouse	40.7398	111.8580	1,328	3.86	CO ₂ , PM _{2.5}	2005	2015	Li-6262	Residential
IMC	Intermountain Medical Center	40.6602	111.8911	1,316	66.0	CO ₂	2016	NA	Li-6262	Commercial
RPK	Rose Park	40.7944	111.9319	1,289	3.25	CO ₂	2009	2015	Li-6262	Residential
DBK	Daybreak	40.5383	112.0697	1,582	5.05	CO ₂ , PM _{2.5}	2004	2015	Li-6262	Rural sagebrush steppe
HDP	Hidden Peak	40.5601	111.6454	3,351	17.1	CO ₂ , CH ₄	2006	2016	LGR UP-GGA	High Elevation / Urban Background
LGN	Logan	41.7616	111.8226	1,392	3.23	CO ₂	2015	NA	Li-6262	Mixed Residential Commercial
HEB	Heber	40.5067	111.4036	1,721	4.20	CO ₂	2015	NA	Li-6262	Residential Developing
SUN	Suncrest	40.4808	111.8371	1,860	4.22	CO ₂	2015	NA	Li-6262	Mid-altitude, Residential
FRU	Fruitland	40.2087	110.8404	2,024	4.04	CO ₂ , CH ₄	2015	NA	LGR UP-GGA	Basin Background
ROO	Roosevelt	40.2941	110.0090	1,585	4.06	CO ₂ , CH ₄	2015	NA	LGR UP-GGA	Basin Residential
HPL	Horsepool	40.1434	109.4680	1,567	4.06	CO ₂ , CH ₄	2015	NA	LGR UP-GGA	Oil and Natural Gas



685 **Table 2: Quality Assurance and Control Flags**

Flag	Descriptor
-1	Data manually removed
-2	System flush
-3	Invalid valve identifier
-4	Flow rate or cavity pressure out of range
-5	Drift between adjacent reference tank measurements out of range
-6	Time elapsed between reference tank measurements out of range
-7	Reference tank measurements out of range
1	Measurement data filled from backup data recording source

**Table 3: CO₂ and CH₄ Measurement Uncertainties with Gaussian window target tank method (U_{pTGT}), target tank (U_{TGT}), analyser precision at 1σ (U_p) and data recovery rates from UUCON and Uintah Basin GHG measurement.**

Site Code	CO ₂ U_{pTGT} (ppm)	CO ₂ U_{TGT} (ppm)	CO ₂ 1σ U_p (ppm)	CH ₄ U_{pTGT} (ppb)	Data Recovery Rate
DBK	0.70	1.04	0.04	NA	0.82
HEB	0.18	0.38	0.04	NA	0.81
IMC	0.35	0.49	0.03	NA	0.71
LOG	0.17	0.51	0.04	NA	0.85
RPK	0.47	0.38	0.10	NA	0.83
SUG	0.31	0.26	0.04	NA	0.80
SUN	0.41	0.54	0.05	NA	0.73
UOU	0.37	NA	0.08	3.3	0.91
FRU	0.28	NA	0.13	2.7	0.86
HDP	0.17	NA	0.10	2.0	0.77
HPL	0.24	NA	0.08	4.2	0.77
ROO	0.18	NA	0.10	1.8	0.81

690

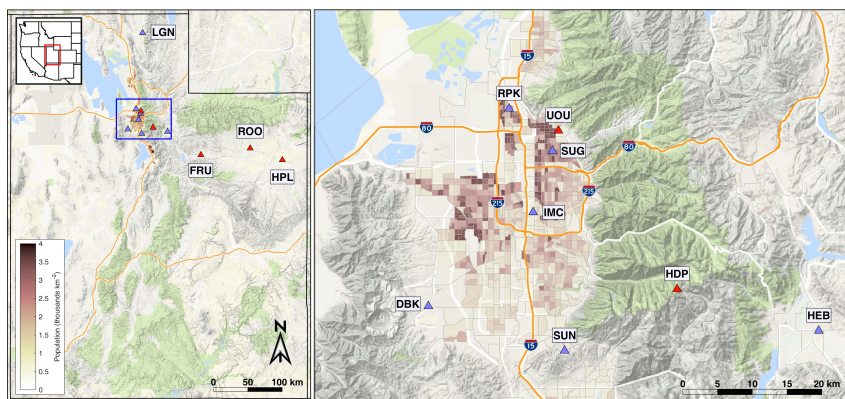


Figure 1: Map showing the location of UUCON and Uinta Basin GHG measurement sites. Left panel shows full distribution of sites in Utah with blue square indicates extent for the right panel. Right panel shows the Wasatch Front and the Salt Lake Valley in detail with population density in thousands per km^2 . Sites equipped with a Li-6262 identified with blue triangle and sites with an LGR UP-GGA identified with red triangle.

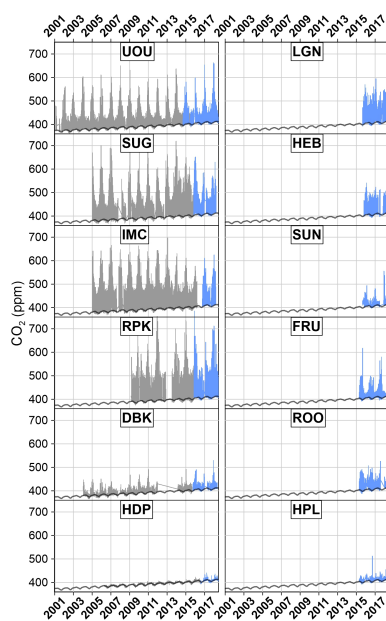


Figure 2: Full record time series of CO₂ measurements from the UUCON and Uintah Basin GHG. Measurement techniques and uncertainty covered in this manuscript indicated by blue with historic data represented in grey. Black line represents regional background as described in Mitchell et al., 2018a.

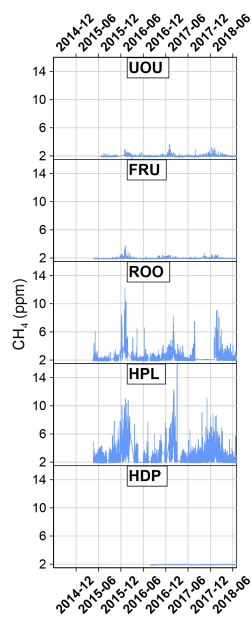


Figure 3: Full record time series of CH₄ measurements from the UUON and Uintah Basin GHG.

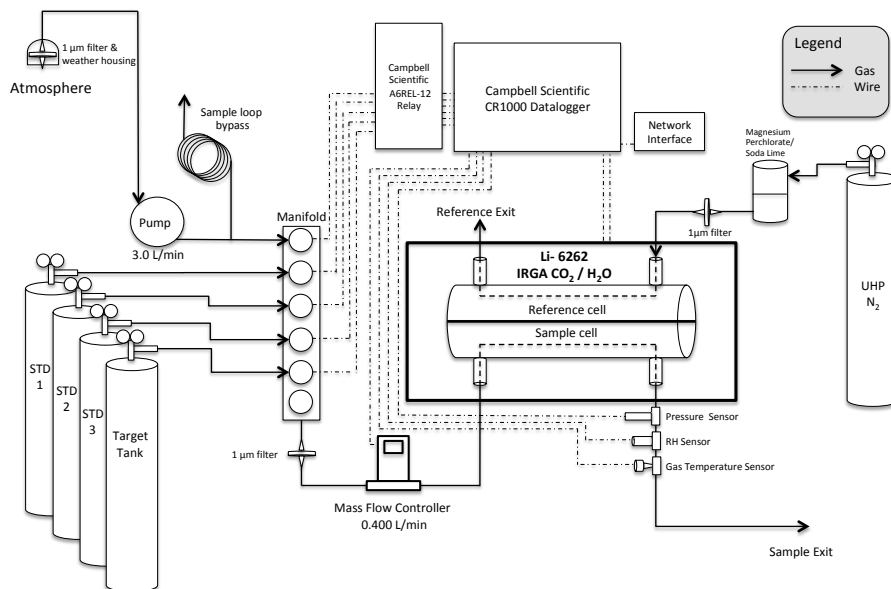


Figure 4: Diagram of UUCON measurement design, not to scale. Sites with this design identified in Fig 1. with blue triangles. STD = Standard Tank.

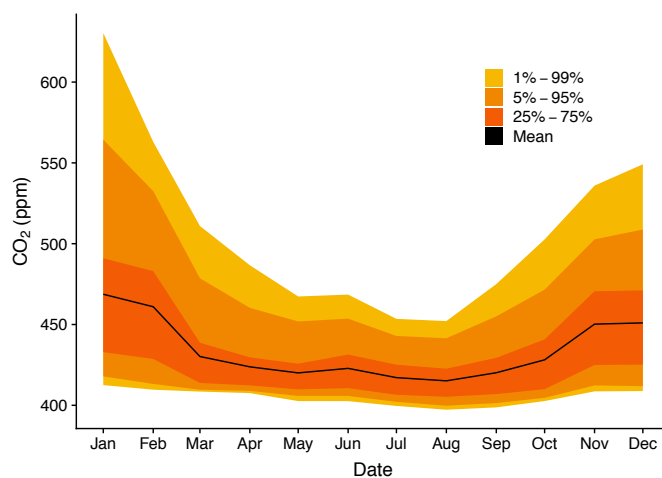


Figure 5: Monthly percentiles of atmospheric observations from SUG over one year, 2017. Note the majority of observations (95th percentile) are greater than 550 ppm CO₂, well beyond the current WMO calibration scale.

700

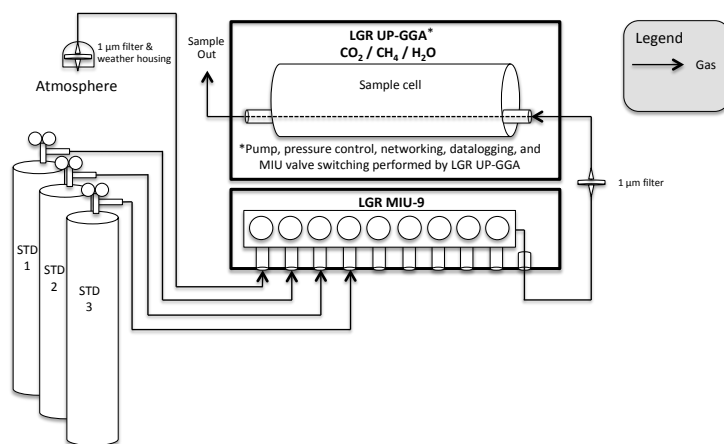


Figure 6: Diagram of Uinta Basin Greenhouse Gas Network measurement design. Sites with this design identified in Fig 1. with red triangles.

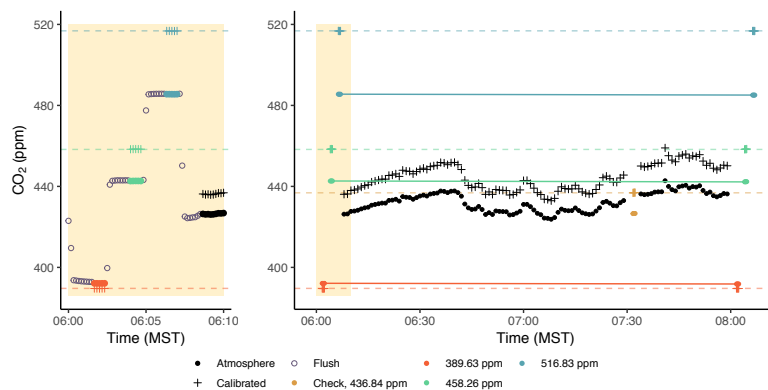


Figure 7: Left panel shows the sequence and timing of a standard calibration period in both the UUCON and Uinta Basin network. Gray open circles indicate the 90 second flushing period observed between each change in gas. Right panel shows a full two hour sample period with calibrations for the UUCON network with linear interpolations, flush periods have been removed. Orange, green, and blue closed circles indicate calibration standard gas and their known CO₂ concentration. Yellow closed circle represents the check tank and its known concentration. Black closed circles indicate pre-calibration atmospheric observations which have been down sampled to one minute averages to reduce over plotting. Plus (+) signs in all colors indicate the post calibrated measurements for the corresponding measurement.

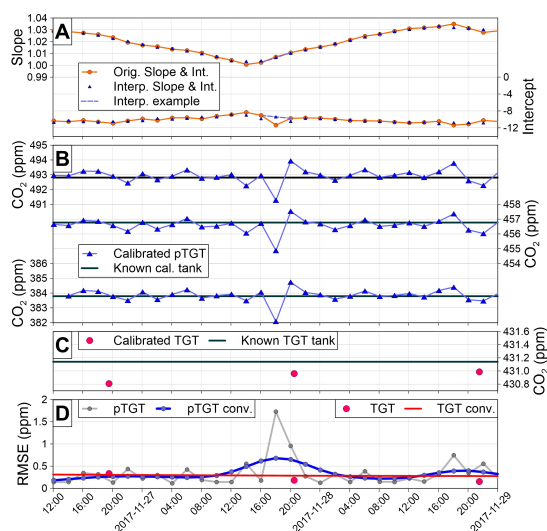


Figure 8: Detailed view of the uncertainty analysis at the IMC site. An example of the interpolation procedure is illustrated for the calibration at 18:00 UTC on November 27, 2017 (see the description in the text). The “pTGT conv.” and “TGT conv.” curves in panel D are the U_{pTGT} and U_{TGT} uncertainty metrics, respectively.

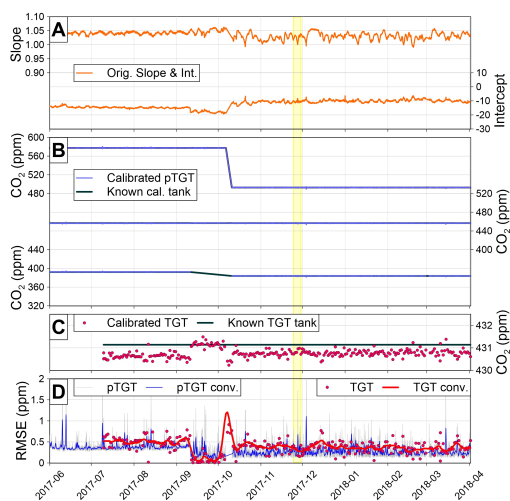


Figure 9: Uncertainty analysis at the IMC site for the time period when a target tank was deployed at the site. The “pTGT conv.” and “TGT conv.” curves in panel D are the U_{pTGT} and U_{TGT} uncertainty metrics, respectively.

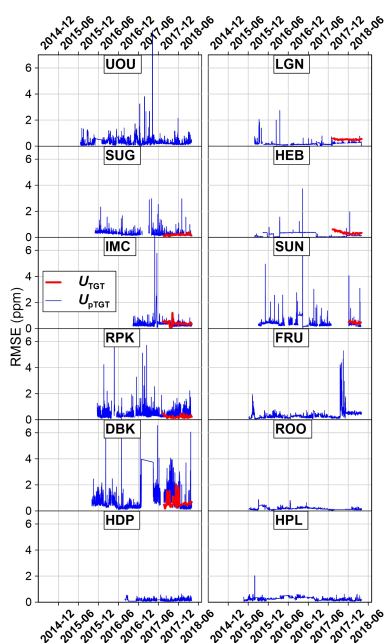


Figure 10: Uncertainty analysis for all of the UUCON sites. The U_{pTGT} and U_{TGT} uncertainty metrics are the same as the “pTGT conv.” and “TGT conv” curves in Fig. 8d and 9d, respectively.

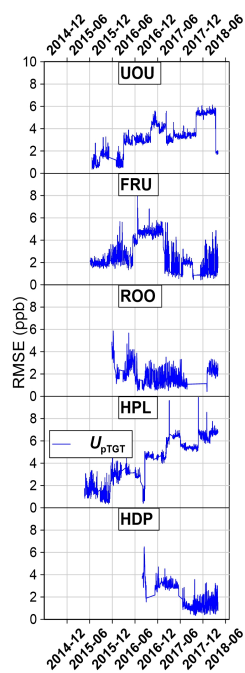


Figure 11: CH₄ Uncertainty analysis. All values reported are the U_{pTGT} uncertainty metrics as shown in Fig. 9d.